Fossil 97:1
Conf. proc.

CONF-9705115--3

THE MICROSTRUCTURE AND MECHANICAL RELIABILITY OF ALUMINA SCALES AND COATINGS

K. B. Alexander, K. Prüßner, and P. F. Tortorelli

Oak Ridge National Laboratory
P. O. Box 2008
Oak Ridge, Tennessee 37831-6376

ABSTRACT

Alumina scales on iron-aluminides (Fe_3Al-based) and NiCrAl-based alloys were characterized in order to develop the knowledge to control the oxidation performance of alloys by controlling the microstructure and microchemistry of their scales. Plasma-deposited amorphous alumina coatings on iron-aluminides were used to study phase transformations, transport processes in the scales and sulfur segregation to the scale/metal interface. It was found, that during heat treatment in the absence of oxidation, amorphous coatings first transform to γ-Al_2O_3 and eventually α-Al_2O_3 nucleates at the scale/metal interface. Sulfur from the Zr-free alloy segregates to the scale/metal interface during heat treatment. Thermally-grown scales on Zr-doped iron-aluminides were compared to those formed after oxidation of a specimen with an alumina coating. Microstructural and gravimetric results showed that the primarily amorphous alumina coating promoted the nucleation and growth of metastable alumina phases, which resulted in more rapid oxidation. The thermally-grown oxide was found on top of the coating. The NiCrAl-based alloys formed columnar alumina scales underneath a layer of mixed oxides. Segregation of alloying elements like Y, Hf and Ta was found at both oxide grain boundaries and scale/metal interfaces.

MASTER

INTRODUCTION

In many high-temperature fossil energy systems, corrosion and deleterious reactions with gases and condensable products in the operating environment often compromise materials performance. The presence of a stable surface oxide can effectively protect the materials from these reactions if the oxides are slow-growing, dense and adherent to the substrate. However, the various factors which control the scale/coating integrity and adherence are not fully understood. Of fundamental interest is the microstructure and microchemistry of the metal/oxide interface as well as oxide/oxide grain boundaries in the scale itself. In alumina scales, segregation of sulfur to the scale/metal interface was found to be detrimental to the oxidation performance, however the presence of reactive elements (RE) such as Y or Zr in the alloy can mitigate the effects of sulfur and thus improve the scale adherence.[1-5] Reactive elements segregate to the oxide/metal

DISTRIBUTION OF THIS DOCUMENT IS UNLIMITED

"The submitted manuscript has been authored by a contractor of the U. S. Government under contract No. DE-AC05-96OR22464. Accordingly, the U.S. Government retains a nonexclusive, royalty-free license to publish or reproduce the published form of this contribution, or allow others to do so, for U.S. Government purposes."

interface and scale grain boundaries and modify the growth mechanisms and the microstructure.[6,7]

The Oak Ridge National Laboratory (ORNL) research described in this paper is being conducted in collaboration with work sponsored by the Department of Energy's Office of Fossil Energy at Argonne National Laboratory (ANL) and Lawrence Berkeley National Laboratory (LBNL) as well as in concert with on-going interactions that are part of the Office of Basic Energy Sciences' Center of Excellence for the Synthesis and Processing of Advanced Materials. The Center of Excellence on Mechanically Reliable Surface Oxides and Coatings includes participants from ORNL, ANL, LBNL, Idaho National Engineering Laboratory (INEL) and Lawrence Livermore National Laboratory (LLNL).

This report will discuss work on the oxidation of iron aluminides, with and without alumina coatings, as well as recent work on the oxidation and segregation behavior of NiCrAl-based alloys. Iron-aluminides (Fe_3Al-type) are known to have good oxidation resistance, if the protective alumina scale can be maintained. It has been shown that small amounts of zirconium significantly reduce the oxidation rate and improve scale adherence in short-term tests at 1000°C.[8,9] Zirconium-containing alloys form unconvoluted, uniform oxide scales with no evidence of spallation during thermal cycling, whereas a significant amount of spallation is observed after thermal cycling of a Zr-free alloy.[8,9] The influence of an applied coating on the oxidation behavior of the alloy should allow the operative transport mechanisms during oxidation to be better examined. The deposition of a plasma-synthesized alumina coating prior to oxidation promoted the growth of metastable aluminas and thus increased the oxidation rate.[10] Both coated and uncoated specimens have needle-like surface morphologies.[10]

Unlike iron-aluminides, NiCrAl-based alloys can result in complex oxide scales with mixed oxides formed in the initial oxidation stages and an alumina layer underneath.[12,13] NiCrAl-based alloys of different compositions, including a commercial superalloy as well as two model alloys were part of the study. Such alloys allow extension of the present work on alumina scales and coatings on Fe-based alloys to a class of Ni-based alloys that are of direct relevance to advanced turbine systems.

EXPERIMENTAL PROCEDURES

The alloys used for the iron aluminide studies were FAL (Fe-28 at. % Al-5 at. % Cr-0.1 at. % Zr + 0.05 at. B) and FA186 (Fe-28 at. % Al-5 at. % Cr), prepared by arc melting and casting. The bulk alloy sulfur content was ~ 40 ppm for both alloys. These alloys were rolled to

a final thickness of between 0.8 and 1.3 mm and rectangular specimens (typically 12 x 10 mm) were prepared from these sheets for coating and oxidation studies.

Oxidation experiments of coated or uncoated iron-aluminides were performed under isothermal and cyclic conditions for 96 h at 1000°C in static air. Gravimetric data were recorded during the cyclic oxidation by exposing coupons in individual pre-annealed alumina crucibles to a series of 24-h exposures. Heat treatments of deposited alumina coatings were performed for 0.5 and 2 h in He at 1000°C.

Alumina coatings on iron aluminides were deposited using a magnetically-filtered cathodic-arc plasma-synthesis process.[13] During the deposition process, the substrate was pulse-biased to a high ion energy (2 kV) in the initial phase of the deposition process to provide atomic mixing of the substrate and film at the interface. A substantially lower energy (0.2 kV) was used to deposit the remaining thickness of the coating.

Three NiCrAl-based alloys of different compositions (commercial superalloy René N5 (from General Electric Aircraft Engines), and ytrrium-doped ternary alloys with similar (NCA-S) as well as higher Cr and Al contents (NCA-H) - Table 1), which form complex oxide scales, were examined after isothermal oxidation in air at 1200°C for 100 h.

Table 1: Composition of NiCrAl-alloys (at %; except S in ppm)

at %	Ni	Cr	Al	Fe	Ta	Hf	W	Re	Si	Co	Mo	Y	Zr	S*	C
Rene N5	64.9	7.8	13.9	0.1	2.1	0.05	1.6	1.0	0.15	7.3	0.9	0.003	0.003	4	0.25
NCA-S	80.1	7.2	12.5	0.01					0.14			0.012		18	0.05
NCA-H	71.2	9.9	18.8	0.01					0.02			0.041		16	0.04

* sulfur contents in ppm

For all experiments, scanning electron microscopy (SEM) was performed on oxidized or heat treated coupons as well as on polished cross-sections through the scale and/or coatings. Field emission gun transmission electron microscopy/scanning transmission electron microscopy (FEG-TEM/STEM) of cross-sectional and plan-view specimens were used for the microstructural characterization of the scales. Energy dispersive x-ray spectroscopy (EDS) with high spatial resolution (1-2 nm probe) was used for the STEM studies of interfacial segregation.

RESULTS AND DISCUSSION

I. Oxidation Studies on Iron-Aluminides

1. Microstructure of Plasma-Deposited Alumina Coatings, As-Deposited

Plasma-deposited alumina coatings which were subsequently used for oxidation and segregation studies of iron-aluminides were primarily amorphous in the as-deposited state (as determined by x-ray diffraction). Auger Electron Spectroscopy (AES) and Rutherford Backscattering (RBS) analyses showed that the films are slightly cation-deficient Al_2O_3.[14] Cross-sectional TEM showed that most coatings had two distinctly different layers: an inner layer which exhibits contrast features perpendicular to the interface and an outer layer, which is featureless (Fig. 1).

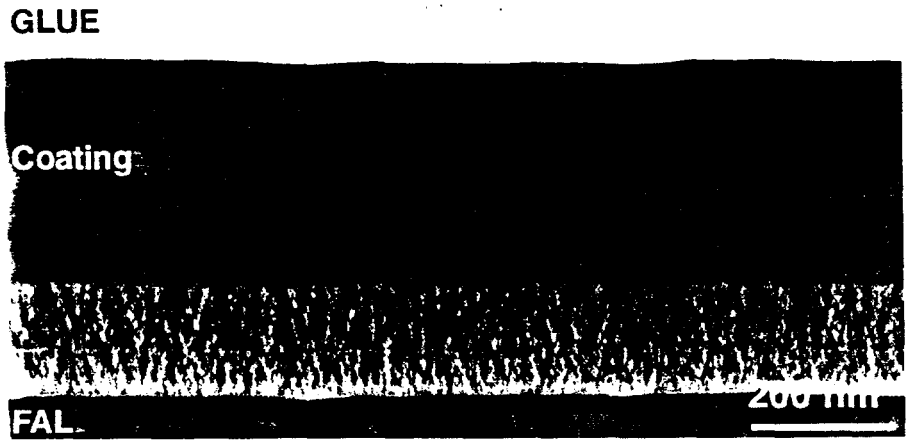

Fig. 1. TEM image of the structure of an as-deposited alumina coating (~ 0.7 μm thick).

The featureless portion was found by selected area diffraction (SAD) to be fully amorphous, whereas some fine-grained γ-Al_2O_3 was found in the inner part of the scale. The difference between the two regions was assumed to correlate with the change in pulse-biasing of the substrate from 2 kV to 0.2 kV during deposition. However, not all the coatings had these two layers. Further investigation of deposition parameter/structure correlations are underway.

2. Microstructural Development and Segregation During Heat Treatment of Alumina Coatings

Previous experiments concerning the segregation of sulfur to the scale/metal interface have only addressed segregation to interfaces between thermally-grown α-Al_2O_3 and an alloy.[3,4,15,16] Since α-Al_2O_3 grows by inward diffusion, the interface is not static but moving into the metal

during oxidation. Therefore diffusion of sulfur to the interface and migration of the interface in the opposite direction are counter-processes. In this study, alumina coatings (0.2 and 0.8 μm thick), plasma-deposited on FA 186, were used to study the segregation of sulfur to a static scale/alloy interface (in the absence of thermal oxidation) and thereby isolate the effect.[16] As-deposited alumina coatings were heat treated in a He-atmosphere at 1000°C (for 0.5 or 2 h) in order to crystallize the initially amorphous coating, while preventing the growth of a thermal oxide scale (if thermal oxidation occurs, oxide needles can clearly be seen on the coating surface by SEM, and this was not observed).

SEM imaging revealed that although the scale/gas interface remained smooth during crystallization, the scale/metal interface showed imprints of distinct oxide grains with associated cracks and cavities as shown in Fig. 2a. The 0.8 μm coating developed a network of cracks and spalled in several areas. The 0.2 μm coating didn't develop these large through-coating cracks. It can be concluded that for the 0.8 μm coating the critical scale thickness for accomodation of thermal and growth/transformation stresses was exceeded.

TEM investigations showed that the heat treatment resulted in the transformation of the coating to metastable alumina (γ-Al_2O_3 and θ-Al_2O_3) and eventually to the nucleation of α-Al_2O_3 at the scale/metal interface (Fig. 3). During the transformation to the metastable aluminas, both interfaces remained fairly flat. The formation of α-Al_2O_3 on the other hand, resulted in roughening of the scale/metal interface. The grains visible as imprints in the top-down SEM images (Fig. 2) could be correlated to faceted grains of α-Al_2O_3 which grew into the alloy. Cavities were formed next to the α-Al_2O_3 (Fig. 3b). Therefore considerable material transport seems to be associated with the phase transformation to α-Al_2O_3 although no thermal oxide growth occurs.

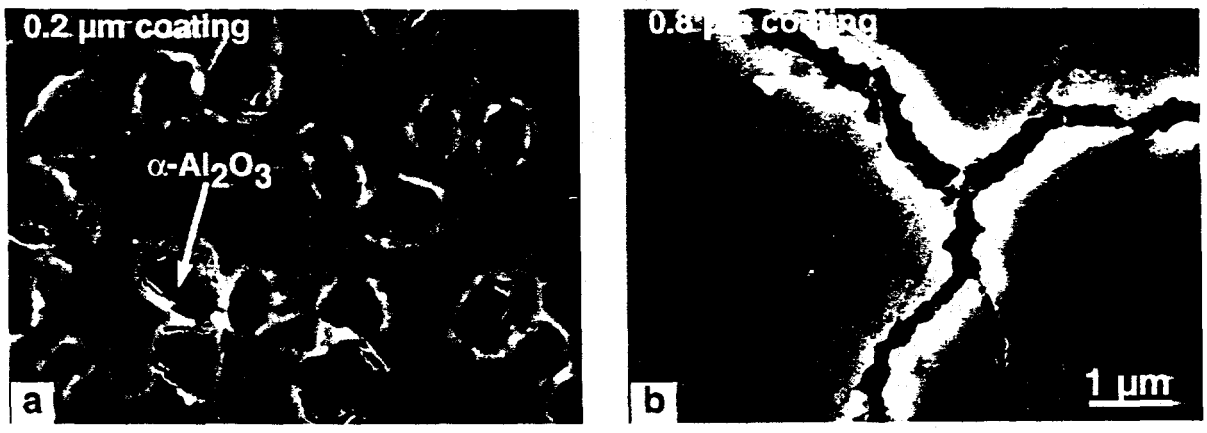

Fig. 2. SEM plan-views of the heat-treated coatings after 2 h in He at 1000°C. (a) 0.2 μm coating, revealing the scale/metal interface (b) 0.8 μm coating, revealing the gas/scale interface.

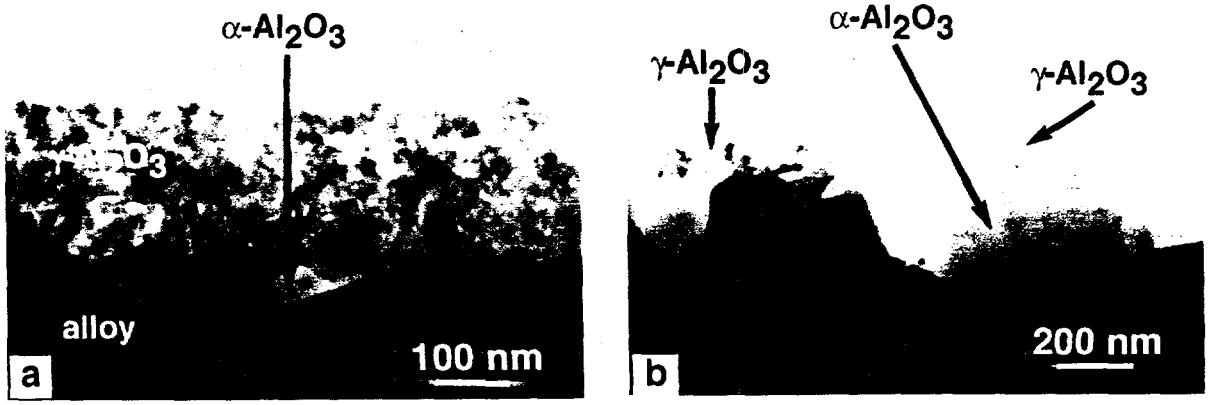

Fig. 3. (a) and (b) TEM cross-sections through heat-treated 0.2 μm thick coating after 2 h in He at 1000°C.

Studies with Auger electron spectroscopy (AES) on FA186/alumina coating interfaces that were freshly exposed by an in-situ scratch-technique, showed that sulfur segregated to the oxide/metal interface during the heat treatment.[16] The sulfur coverage of the interface increased with increasing annealing time and varied in different regions of the specimen. In order to study the correlation between different interface structures and the sulfur level at the interface, high spatial resolution EDS analysis of TEM cross sections was used. Segregation of sulfur was found at α-Al_2O_3/alloy interfaces as well as at γ-Al_2O_3/alloy interfaces (Fig. 4). No interfacial voids were observed in these areas. Quantification of these data is complicated by the roughness of the γ-Al_2O_3/alloy interface (in contrast to the facetted α-Al_2O_3/alloy interface) which made edge-on orientation of the interface impossible. Further analysis is underway to determine if the interfacial sulfur coverage is different for the two microstructures.

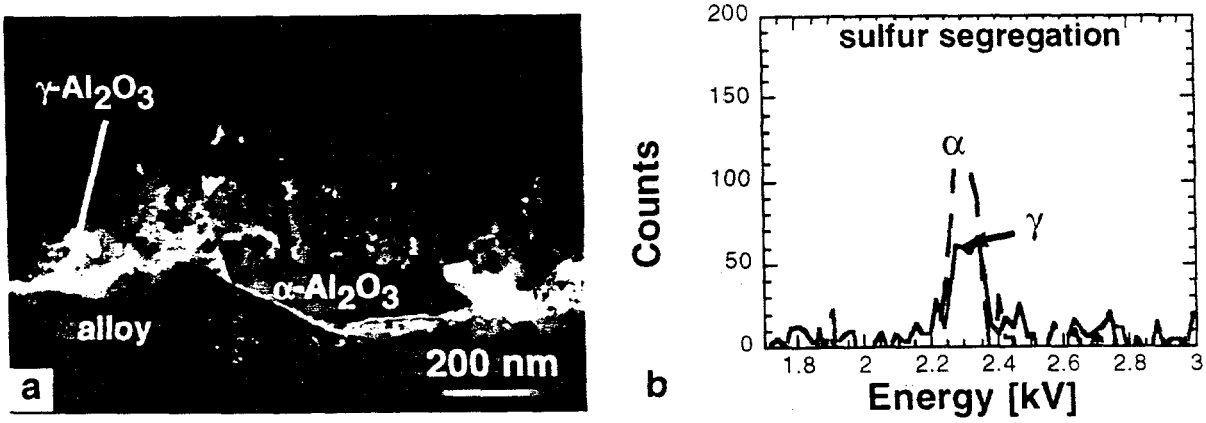

Fig. 4. a) STEM annular dark-field image of γ/alloy and α/alloy interface, b) EDS spectra showing segregation of sulfur at the γ/alloy and the α/alloy interface.

3. Influence of Alumina Coatings on Thermal Oxide Growth on Iron-Aluminides

To study the effect of an alumina coating applied prior to oxidation on the oxidation performance of iron-aluminides, FAL was coated on one side with a 0.1 μm alumina coating and oxidized in air at 1000°C for 96 h. On both the coated and the uncoated sides, oxide scales with a needle-like surface structure were formed (Fig. 5). Both oxide scales were adherent and did not spall. The recorded weight gain demonstrated that the coating increased the rate of oxidation. The oxide scale on the coated side was 1.5-2 μm thick, whereas on the uncoated side it was 0.8-1 μm (Fig. 6).

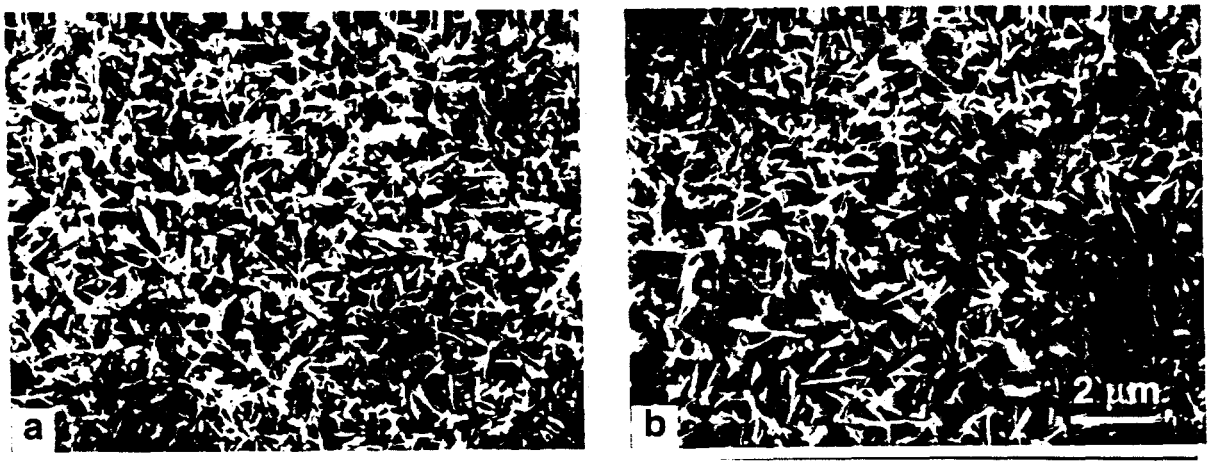

Fig. 5. SEM plan-view of oxidized surfaces exposed 96 h at 1000°C, a) FAL uncoated, b) FAL with 0.1 μm alumina coating.

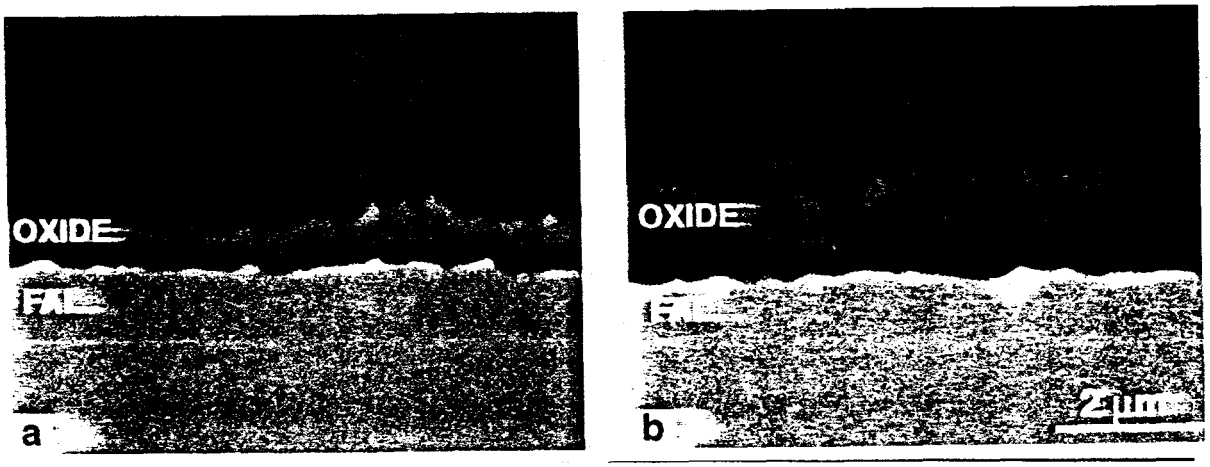

Fig. 6. SEM of polished cross-section after oxidation for 96 h at 1000°C, a) FAL uncoated, b) FAL with 0.1 μm alumina coating.

On the coated side, the original location of the coating can be discerned in the TEM cross-section shown in Fig. 7. The grain size in the area of the original coating is typically 100-150 nm. The grains were identified as nearly dense, equiaxed α-Al_2O_3. The thermally-grown oxide on top of the coating was also α-Al_2O_3 however, it had a much coarser grain structure. Selected-area diffraction showed all portions of the oxide scale, even the oxide needles at the scale/gas interface were α-Al_2O_3, consistent with the pseudomorphic transformation of the transient oxides to α-Al_2O_3 after 96h at 1000°C.

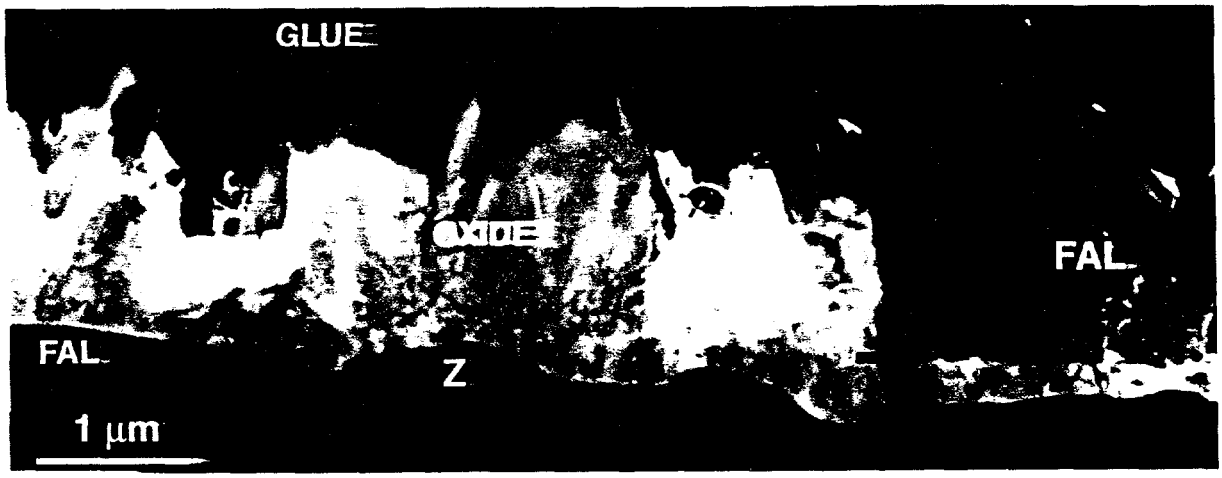

Fig. 7. STEM annular dark-field of coated-and-oxidized (96h at 1000°C) FAL. The location of the original coating is indicated by the arrow.

The identification of the original coating location in the bottom portion of the scale after oxidation implies that most of the scale growth on coated FAL occurred primarily by transport of aluminum through the coating. Although the scale/metal interface on the coated FALwas intact, it roughened during oxidation. This indicates that some transformation of α-Al_2O_3 at the metal/coating interface occurred (similar to that described in the previous section). On the coated surface, Zr-rich metallic particles (typical size: 0.5-1 μm) were found at the scale/metal interface (marked "Z" in Fig. 7). The particles at the scale/metal interface were, compared to the FAL alloy, rich in Zr but contained less Fe and Cr and no oxygen (as determined by STEM/EDS analysis). These particles were not observed at the scale/metal interface in the absence of the alumina coating. The fact that the Zr was not oxidized is consistent with the lack of inward diffusion of oxygen. It is proposed that the amorphous coating promotes the nucleation and growth of metastable alumina phases, resulting in slighly enhanced outwardly-growing oxidation and thicker scales. During the early stages of oxidation, the amorphous coating is therefore ineffective as a protective layer.

Fig. 8. Annular dark-field STEM image of cross-section through scale showing ZrO_2 particles within the scale.

Elemental analysis by EDS showed that zirconium segregated to oxide grain boundaries, both in the initial alumina coating and in the thermally-grown oxide. Segregation of zirconium at the scale/metal interface was also found, both in the coated and uncoated FAL. Auger analysis on metal/oxide interfaces exposed by scratching off the oxide in vacuo revealed the absence of sulfur at the metal/oxide interface.[14] In the portion of the scale near where the amorphous coating was originally located, ZrO_2 particles were found at grain boundaries as well as at the interface between the former coating and the thermally-grown oxide (Fig. 8). The formation of ZrO_2 particles within the oxide on coated-and-oxidized FAL must result from diffusion of zirconium into the coating and subsequent oxidation and/or formation of ZrO_2 during the growth of new oxide.

II. Oxidation Studies on NiCrAl-Alloys

Plan-view images of the three alloys after oxidation are shown in Fig. 9. Figure 10 shows the corresponding cross sections (polished or fractured). The oxide scale on René N5 (~5 μm) consists of columnar α-Al_2O_3 at the bottom (~4 μm) and a mixed layer of spinel (Ni, Co, Ta)(Al, Cr)$_2O_4$ and α-Al_2O_3 (~1 μm) at the top. The mixed oxide layer contains numerous precipitates of Ta,Y,Cr(Hf,Re)-oxides. These are concentrated at the interface between the columnar alumina and the mixed layer. This mixed layer of the scale is prone to spallation.

Similar oxide particles can also be found on the scale surface. Spallation of the complete scale exposing the bare alloy occurs only around particles in the alloy, which consist of Ta,Y,Cr(Hf,Re)-oxide in the center, surrounded by spinel (Ni, Co, Ta) (Al, Cr)$_2O_4$ and α-Al_2O_3. Using STEM/EDS analysis segregation of Ta and Y at oxide grain boundaries both in the alumina and in the spinel was found. Some oxide grain boundaries also exhibited segregation of Hf and Re.

Fig. 9. SEM plan-view images of a) René N5, b) NCA-S and c) NCA-H after oxidation for 100 l at 1200°C.

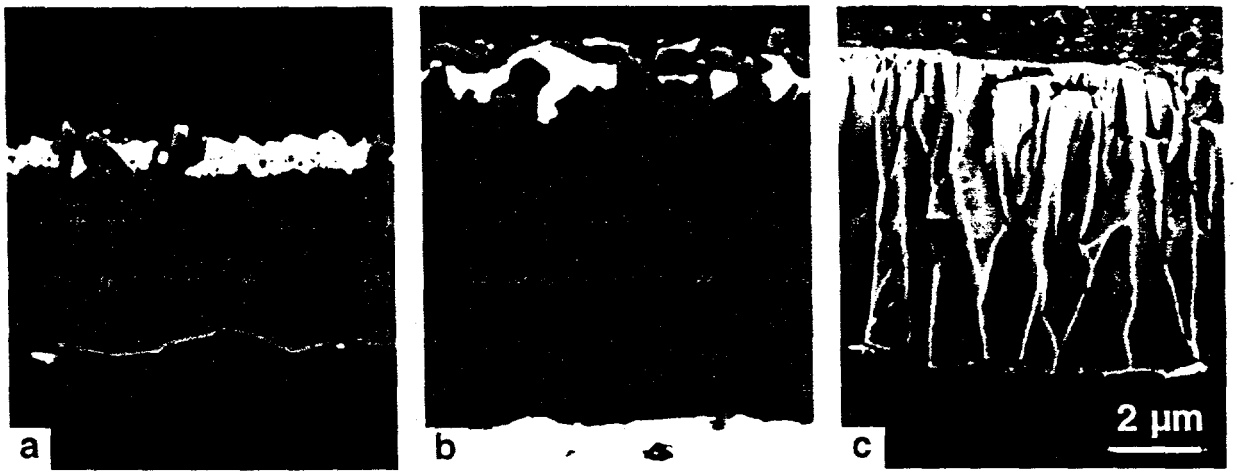

Fig. 10. SEM images of cross-sections of a) René N5, b) NCA-S and c) NCA-H after oxidation for 100 h at 1200°C.

On NCA-S, the scale (~9 µm) consists mainly of columnar Cr-doped α-Al_2O_3. The grain structure of the scale resembles that found on many reactive-element-doped alumina formers (e.g. - Refs. 6, 7, 18) and indicates alumina growth primarily by inward oxygen diffusion.[17] A thin, porous mixed layer of equiaxed spinel ($NiAl_2O_4$) and α-Al_2O_3, as well as some NiO formed on top of the alumina. Over time, NiO transforms to $NiAl_2O_4$ which eventually transforms to α-Al_2O_3; both transformations are pseudomorphic. Spallation of the scale occurred only in a few areas associated with the formation of Y_2O_3, $Y_3Al_5O_{12}$ (garnet) and α-Al_2O_3 at Y-rich alloy grain boundaries. Yttrium-rich oxide particles can be found on the scale surface. Using STEM/EDS analysis, yttrium was also found to be segregated at oxide grain boundaries and at the scale/metal interface.

The NCA-H alloy forms an oxide scale (~8 μm) that consists mainly of columnar Cr-doped α-Al_2O_3. Y-rich oxide particles can be found on the scale surface. The higher level of Y in this alloy results in the formation of Y-rich precipitates at all alloy grain boundaries. Preferential internal oxidation ultimately leads to the formation of Y_2O_3, $Y_3Al_5O_{12}$ (garnet) and α-Al_2O_3 at these grain boundaries. Due to the volume change and thermal mismatch associated with the formation of these phases, almost complete spallation of the oxide scale is initiated at these sites.

SUMMARY AND CONCLUSIONS

Alumina scales on iron-aluminides (Fe_3Al-based) and NiCrAl-based alloys were characterized in order to understand the relationship between the oxidation performance of alloys and the microstructure and microchemistry of their scales. Plasma-deposited amorphous alumina coatings on iron-aluminides were used to study phase transformations, transport processes in the scales and sulfur segregation to the scale/metal interface. It was found, that during heat treatment in the absence of oxidation, amorphous coatings first transform to γ-Al_2O_3 and eventually α-Al_2O_3 nucleates at the scale/metal interface. Sulfur from the Zr-free alloy segregates to the scale/metal interface during heat treatment. Thermally-grown scales on Zr-doped iron-aluminides were compared to those formed after oxidation of a specimen with an alumina coating. Microstructural and gravimetric results showed that the primarily amorphous alumina coating promoted the nucleation and growth of metastable alumina phases, which resulted in more rapid oxidation. The thermally-grown oxide was found on top of the coating. The NiCrAl-based alloys formed columnar alumina scales underneath a layer of mixed oxides. Segregation of alloying elements like Y, Hf and Ta was found at both oxide grain boundaries and scale/metal interfaces. The results from both alloy systems are consistent with previous results on primary alumina-formers. Reactive elements present in the alloy diffuse into the oxide scale and segregate to grain boundaries where they change the diffusion processes resulting in a columnar grain structure of the alumina scale.

ACKNOWLEDGMENT

The authors thank M. Howell for experimental support, B.A. Pint and I.G. Wright for technical discussions and E. A. Kenik for review of the manuscript. This research was sponsored by the Fossil Energy Advanced Research and Technology Development (AR&TD) Materials Program and the Division of Materials Science, U S. Department of Energy, DE-AC05-96OR22464 with Lockheed Martin Energy Research Corp. Research was performed in part with the SHaRE User Facilities at ORNL.

REFERENCES

1. J.G. Smeggil, A.W. Funkenbusch, N.S. Bornstein, Met. Trans. 17A (1986) 923.
2. E. Schumann, J.C. Yang, M.J. Graham and M. Rühle, Oxid. Met. 46 (1996) 37.
3. E. Schumann, Scripta Mater. 34 (1996) 1365.
4. C. Mennicke, E. Schumann, C. Ulrich and M. Rühle, Mat. Sci. Forum (1996) in press.
5. G.H. Meier, F.S. Pettit and J.L. Smialek, Mat. Corr. 46 (1995) 232.
6. B.A. Pint, Oxid. Met. 45 (1996) 1.
7. B.A. Pint and K.B. Alexander, submitted to J. Electrochem. Soc.
8. P.F. Tortorelli and K.B. Alexander, pp. 247-56 in *Proc. Ninth Annual Conf. Fossil Energy Materials*, N.C. Cole and R.R. Judkins (comp.), CONF-9505204, U. S. Department of Energy, August 1995.
9. P.F. Tortorelli and J.H. DeVan, pp. 257-70 in Processing, Properties, and Applications of Iron Aluminides, J.H. Schneibel and M.A. Crimp (eds.), The Minerals, Metals, and Materials Society, Warrendale, PA, 1994.
10. K.B. Alexander, K. Prüßner, P.Y. Hou and P.F. Tortorelli, 3rd Int. Conf. Microscopy of Oxidation, The Institute of Metals, London(1996) in press.
11. C.S. Giggins and F.S. Pettit, J. Electrochem. Soc. 118 (1971) 1782.
12. A. Kumar, M. Nasrallah and D.L. Douglass, Oxid. met. 8 (1974) 227.
13. I.G. Brown and Z. Wang, Proc. Ninth Annual Conf. Fossil Energy Materials, U.S. Department of Energy (1995) 239.
14. P.Y. Hou, Z. Wang, K. Prüßner, K.B. Alexander and I.G. Brown, 3rd Int. Conf. Microscopy of Oxidation, Cambridge (1996) in press.
15. P. Fox, D.G. Lees and G.W. Lorimer, Oxid. Met. 36 (1991) 491.
16. K. Prüßner, E. Schumann and M. Rühle, pp. 344-56 in Fundamental Aspects of High Temperature Corrosion, D. A. Shores, R. A. Rapp, and P. Y. Hou (eds.), Proc. Vol. 96-26, The Electrochemical Society, Pennington, New Jersey, 1997.
17. B. A. Pint, pp. 74-85 in Fundamental Aspects of High Temperature Corrosion, D. A. Shores, R. A. Rapp, and P. Y. Hou (eds.), Proc. Vol. 96-26, The Electrochemical Society, Pennington, New Jersey, 1997

DISCLAIMER

This report was prepared as an account of work sponsored by an agency of the United States Government. Neither the United States Government nor any agency thereof, nor any of their employees, makes any warranty, express or implied, or assumes any legal liability or responsibility for the accuracy, completeness, or usefulness of any information, apparatus, product, or process disclosed, or represents that its use would not infringe privately owned rights. Reference herein to any specific commercial product, process, or service by trade name, trademark, manufacturer, or otherwise does not necessarily constitute or imply its endorsement, recommendation, or favoring by the United States Government or any agency thereof. The views and opinions of authors expressed herein do not necessarily state or reflect those of the United States Government or any agency thereof.

DISCLAIMER

Portions of this document may be illegible in electronic image products. Images are produced from the best available original document.